

Chapter 7

Photodissociation of Bromine

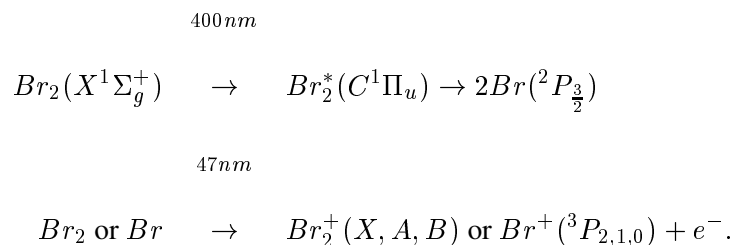
7.1 Introduction

As a chemical bond is broken (or made), the electron distribution changes on an ultrafast time scale to accommodate the moving nuclei. To understand how this electron distribution changes with time is not only of fundamental interest but will also provide critical information on the specific chemical system and the dynamics of the ensuing reaction. In a simple system (Br_2), we observe a real time signature of a bond breaking in a gas phase molecule by measuring the kinetic energies of the ejected electrons as a function of pump-probe time delay. The changing electron distribution of the dissociating molecule is reflected in the binding energies of the electrons themselves and thus is detectable in its valence and core level soft x-ray photoelectron spectra.

Bromine was chosen as the initial sample for study for a number of reasons, the most important being that it is a simple system with a straightforward static photoelectron spectrum, and that it also has a relatively strong absorption cross-section at 400 nm ($5 \times 10^{-19} \text{ cm}^2$). The results presented here demonstrate that a number of complex issues exist even in a simple system, including above threshold cross-correlation features vs. transient signals, the onset of atomic photoelectron signals, multiple final ion states, and issues of atomic and transient state ionization cross-sections. Here I outline the details of the results for the photodissociation of Br_2 and discuss the analysis of the data and possible interpretations.

7.2 Pump-Probe Photoelectron Spectra in Br₂

The photodissociation scheme for probing the time-resolved dynamics of Br₂ is as follows:



The 400 nm pump pulse excites the neutral Br₂ molecule to the $C^1\Pi_u$ dissociative state, and at time delays ranging from -500 fs to +1 ps the 17th harmonic probes the electron distribution by photoelectron spectroscopy. Figure 7.1 gives the potential energy curve diagram of Br₂/Br₂⁺ taken from refs. [65] and [61]. This simplified diagram illustrates 4 different processes that are observed in the data presented here. These include: (1) the background signal from ground state ionization by the 17th harmonic, (2) the cross-correlation signals at t=0, (3) ionization of the excited state wavepacket before dissociation is complete, and (4) the ionization of the final Br atom products. These different processes are discussed in more detail below. The diagram shows only the X and C electronic states of neutral Br₂ and the X and A states of Br₂⁺ for simplicity, since these are the important electronic states involved in the photodissociation and ionization processes in the pump-probe experiment.

Figure 7.2 expands three pump-probe spectra from the same dotted box in Fig. 5.4, corresponding to pump-probe delays of -500 fs, -100 fs, and +500 fs. In Fig. 7.2, the background between the molecular peaks increases due to saturation of the detector on the main peak in order to amplify the small pump-probe signal. The spectrum corresponding to $\Delta t = -500$ fs is the background signal that appears with the soft x-ray pulse coming before the 400 nm pump pulse. The signal in the $\Delta t = -100$ fs spectrum at 7.5 eV binding energy is indicative of a cross-correlation, by means of a two-photon (400 nm + 17th harmonic pulses) ionization of the Br₂

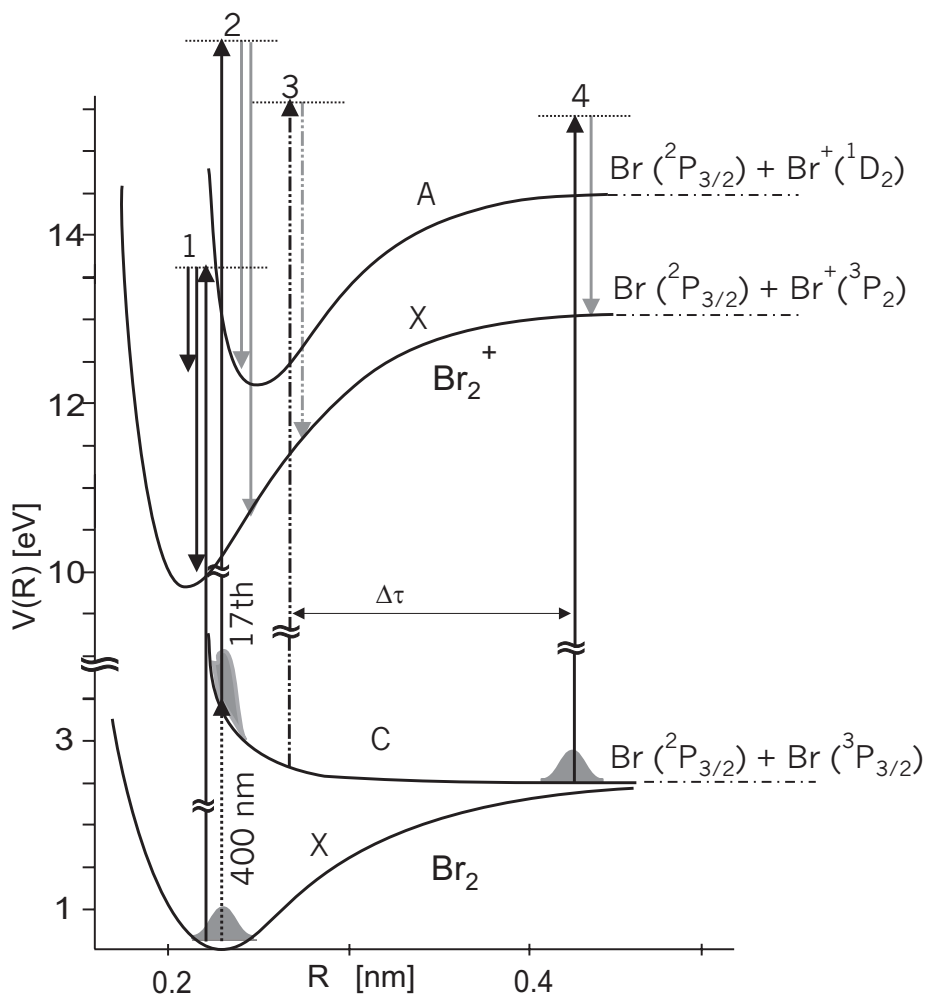


Figure 7.1: A simplified potential curve diagram illustrating the pump-probe sequence and resulting photoelectrons. **Process 1:** Ground state absorption of the 17th harmonic resulting in photoelectrons leaving Br_2^+ in both the X and A state (B ion state not shown). **Process 2:** Two photon ionization with the 400 nm + the 17th harmonic centered at $t=0$. **Process 3:** Ionization with the 17th harmonic from the excited C state of Br_2^* at a positive time delay (but before dissociation is complete). **Process 4:** After the dissociation is complete, the Br atoms are ionized by the 17th harmonic. The total energy of the probe laser is decreased for simplicity and size of the diagram.

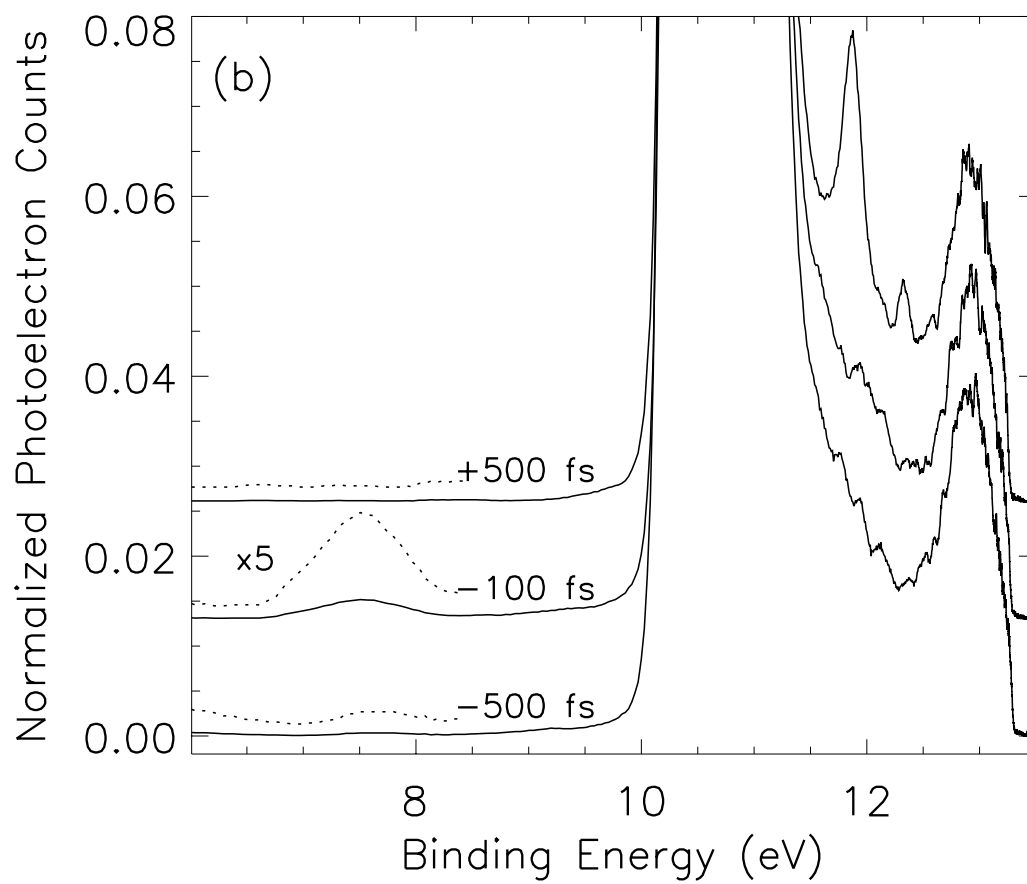


Figure 7.2: Three pump-probe spectra of Br₂: $\Delta t = -500$ fs (background), -100 fs (cross-correlation signal), and $+500$ fs (Br atom signal). The spectra are displaced vertically for clarity.

molecule. There are two processes which could result in a photoelectron signal at this energy. First, the 400 nm pulse promotes the wavepacket resonantly to the excited state and then the wavepacket is instantaneously ionized by the 17th harmonic. Second, a purely above threshold ionization process could also occur (similar to the case in Xe), where the 17th harmonic ionizes Br₂ and the 400 nm adds on to the ionization energy at $t = 0$. If the signal is due to the wave packet on the dissociative state, then the photoelectron spectra of the dissociative state is observed directly. Due to issues discussed later in this chapter, it is most likely a combination of the two processes. This cross-correlation feature is also useful as an internal determination of the temporal width of the soft x-ray pulse. The cross-correlation signal should be a doublet, mirroring the one-photon ionization molecular peak leading to the X state of Br₂⁺, however, it appears at a photoelectron energy where the magnetic bottle resolution is less than the doublet separation. Cross-correlation features are also expected where the Br₂⁺ is produced in the A and B states. The A state cross-correlation signal has been observed, appearing as a small shoulder on the low binding energy side of the X state background peak. Although the B state signal has not yet been observed, it is expected to be of a similar binding energy as the atomic signal, further complicating the spectrum. An expanded photoelectron spectrum highlighting the cross-correlation features is shown in Fig. 7.3. A signal in between the cross-correlations leading to the X state and the A state of the ion is attributed to the excited state wavepacket being ionized after sliding down the dissociative curve, which is discussed in more detail later in the chapter. Lastly, in the $\Delta t = +500$ fs spectrum, photoelectron peaks from the Br atom are observed at the expected binding energies while the cross-correlation signal is no longer present. This atomic signal persists at long time delays ($\Delta t = 100$ ps) compared to the time scale of the dissociation dynamics ($\Delta t < 500$ fs).

In Fig. 7.4, several photoelectron spectra are normalized and the background molecular signal is subtracted so that only the time-correlated signal remains. Figure 7.4 show a series of pump-probe spectra in the relevant energy ranges where the time-correlated peaks of the cross-correlation and atomic peaks appear. The small shift of the photoelectron spectra to lower

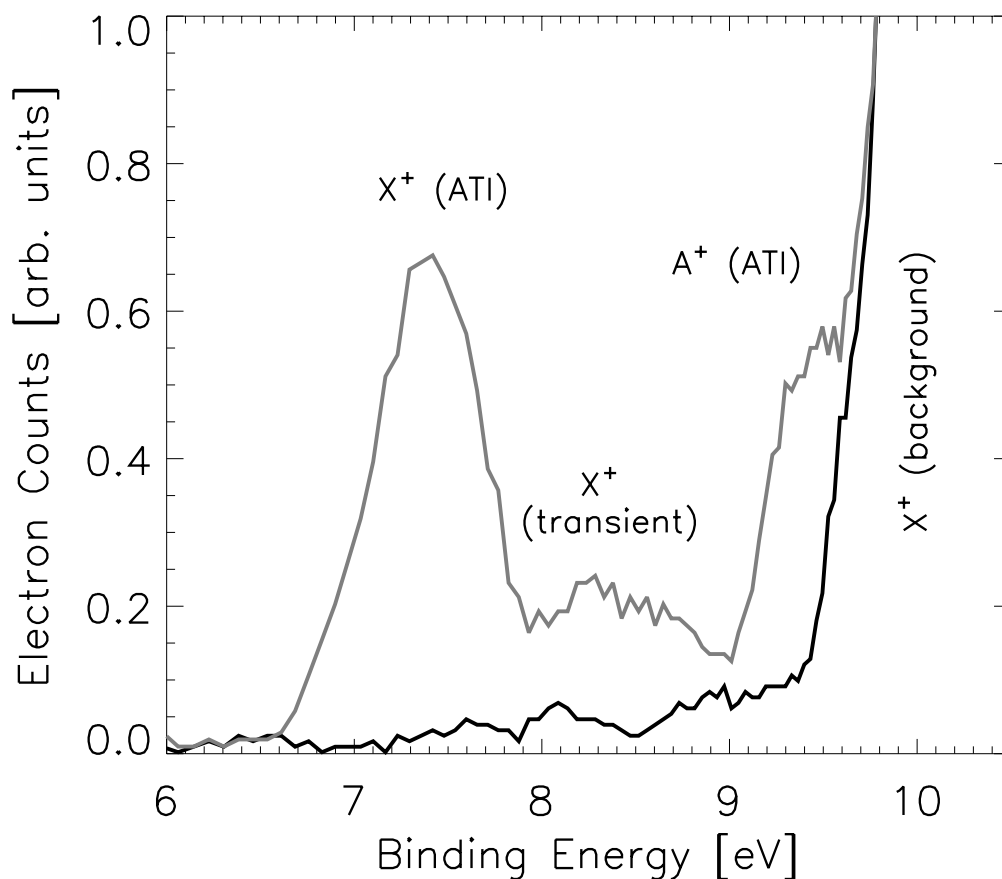


Figure 7.3: An expanded region of the photoelectron spectrum of Br_2 at $\Delta t \sim 30$ fs (gray line) and background at $\Delta t \sim 300$ fs (black line) showing the cross-correlation features. The feature at 7.4 eV binding energy is the above threshold ionization resulting from the overlap of the 17th and 400 nm pulses where the Br_2^+ is left in the ground X state. The shoulder roughly centered at 9.4 eV is a similar signal, only the Br_2^+ is left in the excited A state. The signal at ~ 8.5 eV is attributed to the ionized excited state wavepacket as it is sliding down the dissociative curve.

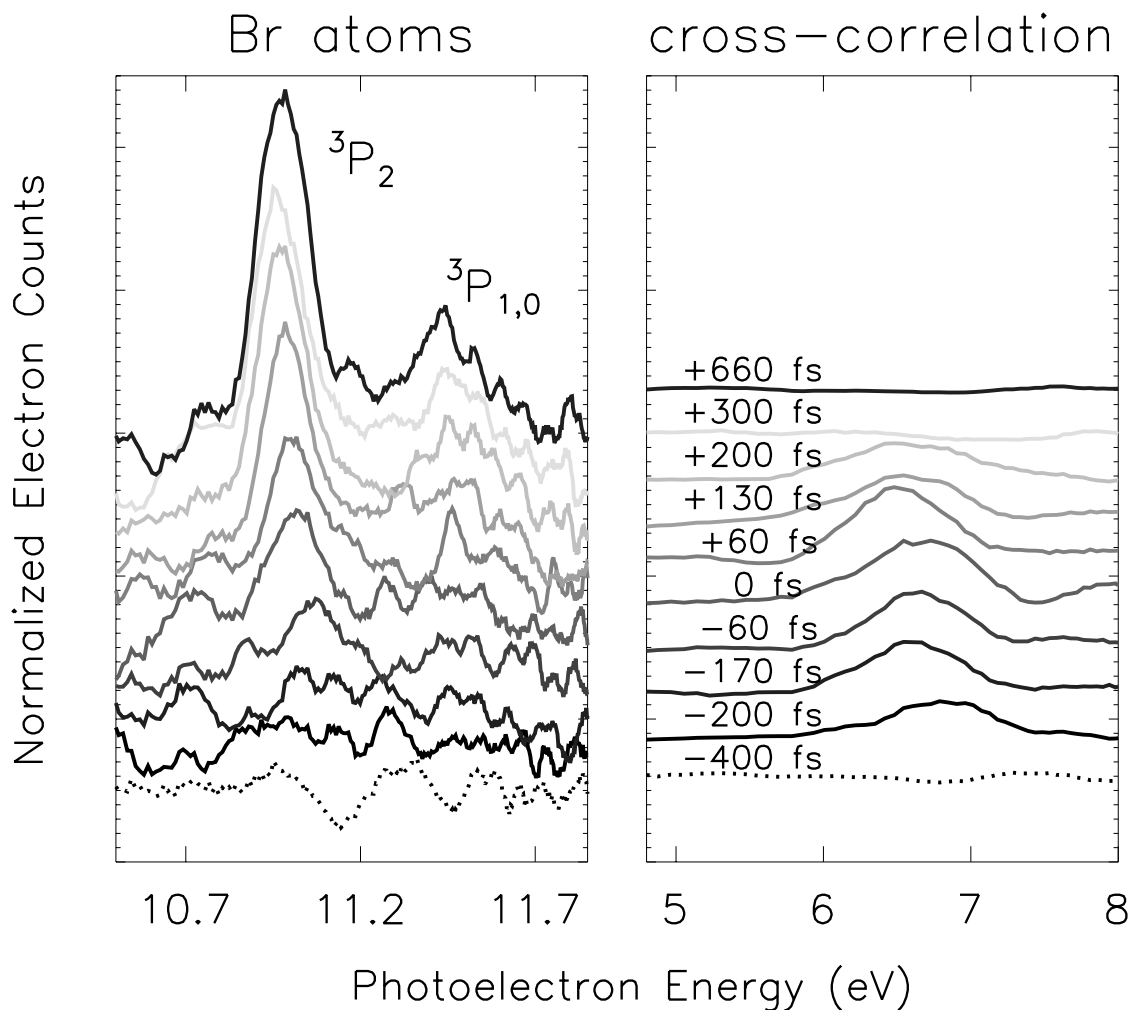


Figure 7.4: Normalized, subtracted pump-probe spectra of Br_2 in the cross-correlation time region (left). The spectra are displaced vertically for clarity. The panel on the right shows the appearance of the Br atom peaks in the photoelectron spectra. The two peaks in the photoelectron spectrum are due to spin-orbit coupling in the final Br^+ state. Numbers on the vertical scale are pump-probe delay in femtoseconds.

binding energies with increasing time delay is the result of a linear chirp in the soft x-ray pulse that is not compensated by the grating pair. From the data, it is clear that the atomic peaks rise very quickly, although their onset is delayed slightly with respect to the cross-correlation.

7.3 Time-traces of cross-correlation and Br atom signals

The delay between the center of the cross-correlation and the atomic rise is more clearly seen in Fig. 7.5 where the total photoelectron counts under both the cross-correlation peak and the atomic peaks are plotted vs. pump-probe delay. The solid line represents a Gaussian fit to the cross-correlation data points (filled circles) corresponding to the following equation:

$$S(t) = S_0 + A \times \exp \left[-4 \ln 2 \left(\frac{(t - t_0)}{\sigma_{fwhm}} \right)^2 \right]. \quad (7.1)$$

$S(t)$ is the total signal, S_0 is the y offset of the curve (or constant background signal), A is the peak height, t_0 is the time value of the peak of the curve, and σ_{fwhm} is the full width at half maximum of the Gaussian curve. The fit to the data gives a full width at half maximum of 300 ± 14 fs and peak time $t_0 = 0 \pm 14$ fs. The dotted line is a fit to the rise of the total atomic signal (diamonds) with a smoothed step function given by the following equation:

$$S(t) = \frac{1}{2} \operatorname{erf} \left(\frac{(t - \tau_{step}) 2\sqrt{\ln 2}}{\sigma_{fwhm}} \right) + \frac{1}{2}. \quad (7.2)$$

$S(t)$ is the total signal, τ_{step} is the average time delay between a hypothetical instantaneous photon absorption and product atom formation, and σ_{fwhm} is the full width at half maximum of the above mentioned Gaussian [66]. The best fit to the data was found with $\sigma_{fwhm} = 250 \pm 13$ fs and $\tau_{step} = 40 \pm 13$ fs. The discrepancy between the σ_{fwhm} values obtained from the Gaussian function and the step function could indicate that the atomic rise is less effected by the wings of the cross-correlation between the 400 nm and soft x-ray pulses, and the time resolution is determined by the middle part of the pulse, which would give a smaller value for σ_{fwhm} . However, the dashed line is the same step function fit to the atomic data, only with σ_{fwhm} fixed at the cross correlation value of 300 fs. The value of τ_{step} for the dashed curve is 37 ± 13 fs, well within experimental error for the earlier value.

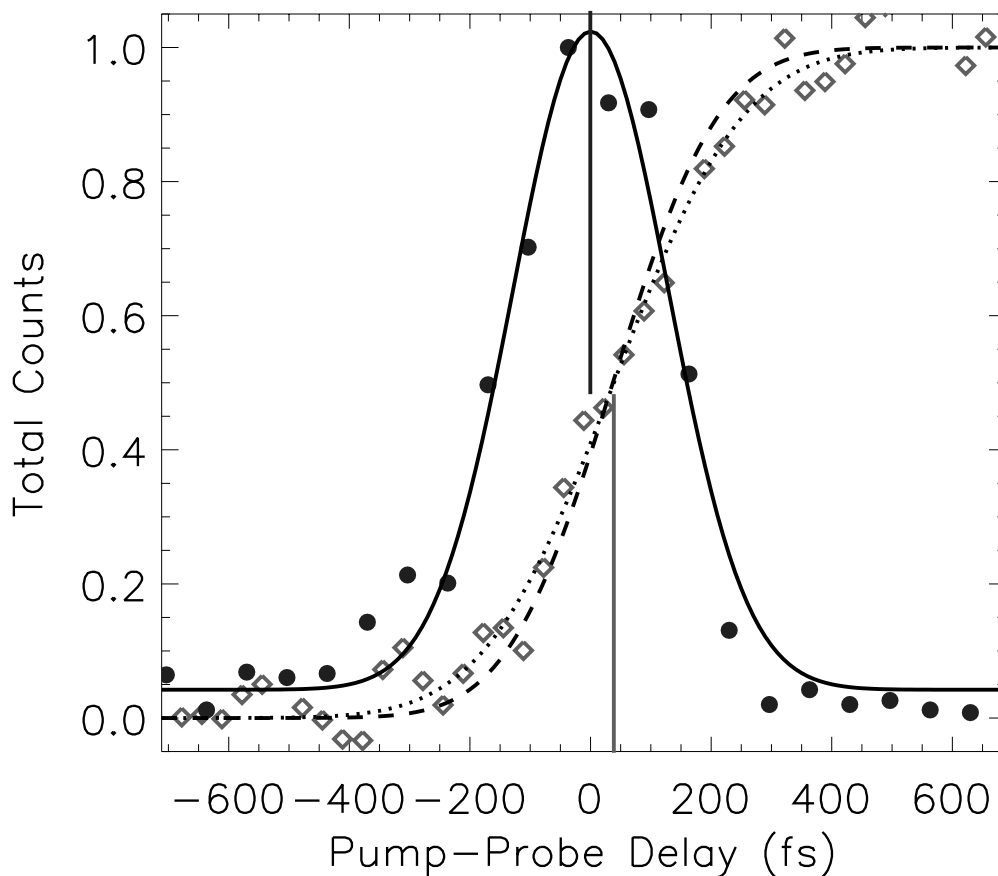


Figure 7.5: Total counts from the cross-correlation peak and the atomic peaks from Fig. 7.4 and additional time delay data not shown are plotted as a function of pump-probe delay between the 400 nm pump and the 17th harmonic probe. The cross correlation signal is fit with Gaussian function of width ~ 300 fs and the atomic rise is fit with a step function described in the text. The dotted line fit of the step function allows both τ_{step} and σ_{fwhm} to be variables, while the dashed line fit fixes σ_{fwhm} to 300 fs. The solid lines designate the time delay between the center of the cross-correlation trace and the 'step' of the error function used to fit the rise in atomic signal.

A similar delay is seen when using the 19th harmonic as the probe, which has a shorter duration as discussed in chapter 6. The cross-correlation and atomic signals are about 50% weaker when using the 19th harmonic as the probe compared to the data taken with the 17th harmonic. The time traces for the 19th harmonic data set are shown in Fig. 7.6. In this data set, the cross-correlation is narrower, with a FWHM of 204 ± 17 fs and t_0 of 0 ± 17 fs resulting from the Gaussian fit. There is also a significant shoulder seen in the data at negative times. With a shorter soft x-ray pulse, some irregularities in the temporal profile could indicate structure in the spectral or spatial profile of the soft x-ray pulse, probably caused during the harmonic generation processes itself. The atomic data with the 19th harmonic is more scattered than in the case of the 17th harmonic due to decreased atomic signal. The shoulder of the cross-correlation peak also shifts the atomic curve. Atoms created at the peak of the local maximum (shoulder) will shift the τ_{step} to earlier times. While the parameters for the step function fit to the atomic data have large errors ($\tau_{step} = 36 \pm 21$ fs and $\sigma_{fwhm} = 367 \pm 45$ fs), the trend remains same as in the 17th harmonic data. Again, the dashed line in Fig. 7.6 is from equation 7.2, except with the σ_{fwhm} held at 204 fs. The value of τ_{step} then becomes 30 ± 20 fs.

This 40 fs delay of the onset of the atomic signal with respect to the center of the cross-correlation suggests a very fast dissociation time for the Br_2 molecule. A first order approximation of the dissociation time of Br_2 is accomplished by using a total energy equation and calculating the integral under the $^1\Pi_u$ dissociative curve. From Ref. [67], I use equation (9) as the estimate of the dissociative curve, derived based on experimental lifetime measurements and valid in the region $2.5 \leq R \leq 3.5$ Å. The equation is as follows:

$$U(R) = U_{limit} + \left(\frac{1.594 \times 10^7}{R^{9.384}} \text{cm}^{-1} \right) \quad (\text{see Fig. 7.7(a)}). \quad (7.3)$$

where $U(R)$ is the potential energy as a function of R , the internuclear distance, and U_{limit} is the atomic limit with respect to the ground state neutral well. The 9.384 power represents the steep repulsion of the dissociative curve. By generating a series of points along this curve, the integral under the curve is determined numerically. First, the integrand relating time of dissociation (t)

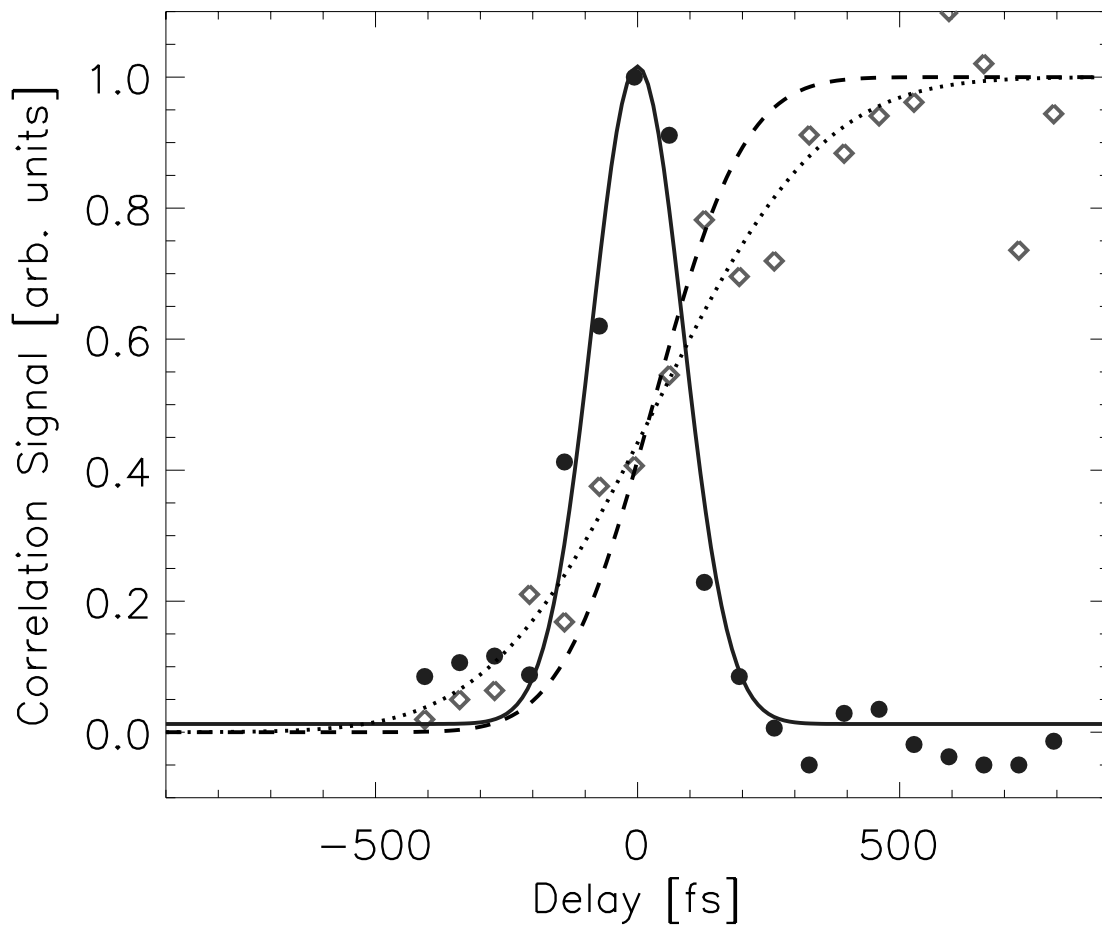


Figure 7.6: A similar plot as Fig. 7.5 except using the 19th harmonic as a probe. The cross-correlation signal has a FWHM of 204 ± 17 fs and t_0 of 0 ± 17 fs, and the fit to the atomic rise gives $\tau_{step} = 36 \pm 21$ fs and $\sigma_{fwhm} = 367 \pm 45$ fs (dotted line) and the dashed line is a fit holding σ_{fwhm} at 204 fs, and τ_{step} then becomes 30 ± 20 fs.

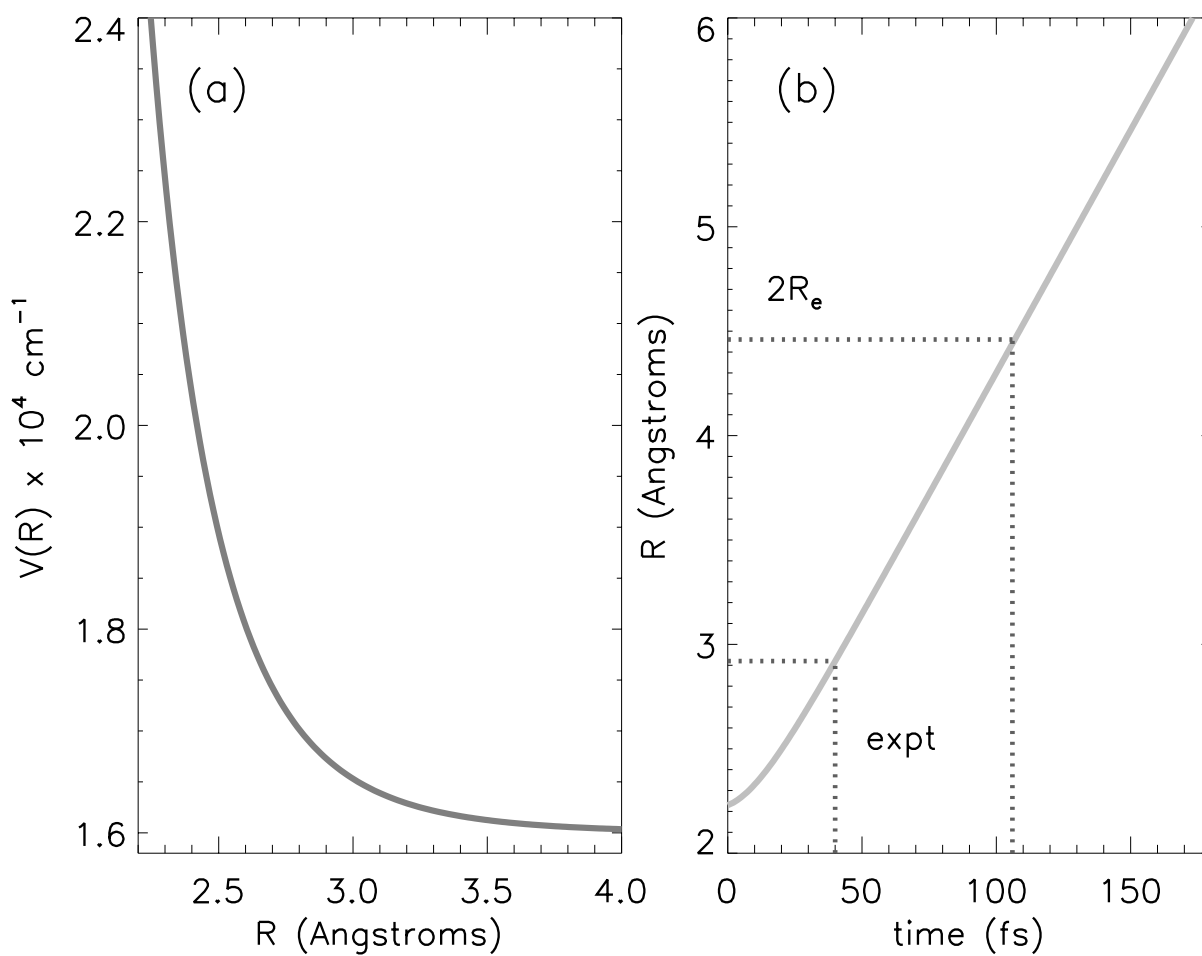


Figure 7.7: (a) The $C^1\Pi_u$ dissociate of neutral Br_2 given by equation 7.3 (b) A curve representing the integral of (a) in fs per \AA . The experimental result of 40 fs implies a bond distance of $\sim 3 \text{ \AA}$, while a bond distance of $2R_e$ occurs at a time of 105 fs.

to internuclear distance (R) is calculated from the following equations:

$$E_{total} = E_{KE} + E_{PE}$$

$$E_{total} = \frac{1}{2}\mu \left(\frac{R}{t}\right)^2 + U(R).$$

Since t and R are the variables, I rearrange to solve for dt as a function of dR :

$$dt = \left(\sqrt{\frac{2}{\mu}(E_{total} - U(R))} \right)^{-1} dR \quad (7.4)$$

where E_{total} (in Joules) is the total energy put into the system, E_{KE} is the kinetic energy of the atoms with respect to the center of mass, E_{PE} is the potential curve given by equation 7.3 (converted to Joules), and μ is the reduced mass of Br_2 in kg. Numerical integration of the above integrand results in the curve in Fig. 7.7(b), relating time and internuclear distance (after conversion to fs and \AA).

This calculation reveals that in 40 fs the Br-Br separation will have reached $\sim 3\text{\AA}$ from an initial equilibrium bond distance of $R_e = 2.23\text{\AA}$ in the ground state [65]. This elongated bond distance is in a regime where atomic behavior cannot be ruled out, but it is still closer to R_e than $2R_e$, a bond distance where it is safe to assume the bond is completely broken. Shortly after the two pulses begin to overlap, there is always some percentage of the soft x-ray probe pulse that follows the much shorter 400 nm pump pulse. With an estimated dissociation time of ≤ 40 fs, some signal due to atoms in the interaction region should appear at very early time delays. However, one might also expect a broad peak in the atomic region at early time delays, with signal coming from the dissociating wavepacket over several regions of the dissociative curve. Then at later time delays, the atomic peak should become narrower as the dissociation is nearly complete. The results presented in Fig 7.4 show no visible broadening of the atomic peak at early time delays. However, such a broadening of the signal could be wider than 1 eV considering the energy scale covered by the $^1\Pi_u$ curve. If this is the case, the broad signal might be impossible to detect above the background parent molecule signal level [see Fig. 7.2].

Another explanation of the observations is the possible existence of an ion-induced dipole potential curve that would almost mirror the neutral dissociative curve, except with a

very shallow well. This could cause the photoelectron feature arising from the dissociating wavepacket to appear at a nearly constant energy. This could also account for the lack of shift of the atomic Br peaks that is observed. The discrepancy in the σ_{fwhm} values from the cross-correlation and the convoluted step function fit (especially in the data taken with the 19th harmonic) lends some validity to this idea. It is perhaps not complete to describe the dissociation dynamics as an instantaneous step function. The longer σ_{fwhm} from the step function fit of the 19th harmonic data (where the time resolution is the best) could indicate that another process is going on, creating a longer time delay than the width of the cross-correlation.

7.4 Ionization of the excited state wavepacket

The analysis of the dissociative state photoelectron spectra is complicated by multiple final states of the ion and multiple cross-correlation features. If the ion is left in the X state after ionization at a dissociative bond distance of $\sim 2.4 \text{ \AA}$, a photoelectron peak between the two observed cross-correlation peaks (that leave the Br_2^+ in the X state and A state) is expected. The small peak in Fig. 7.3 at $\sim 8.5 \text{ eV}$ binding energy could arise from the dissociating wavepacket. This signal rises and decays on the appropriate time scale for it to be a dissociative state photoelectron feature. This transient signal is analyzed more closely as demonstrated in Fig. 7.8. Four time traces are taken from the pump-probe photoelectron spectra with the 400 nm pump and 17th harmonic probe. The features are shifted in electron kinetic energy, but they are collected here on one pump-probe time trace. The black line is the cross-correlation leaving the Br_2^+ ion in the X state (corresponding to the signal from 6.5 to 8 eV binding energy in Fig. 7.3), the dotted line is the cross-correlation leaving the ion in the A state (9-9.5 eV), the medium gray line is the transient signal from 8-9 eV, and the light gray line is a random sampling of background signal from 5-6 eV binding energy. The transient signal clearly rises above the random noise trace and also has a similar Gaussian shape and width as the cross-correlation traces. This is consistent with what would be expected if the excited state wavepacket were ionized after moving out on the dissociative curve. As energy is deposited into kinetic energy of the atoms,

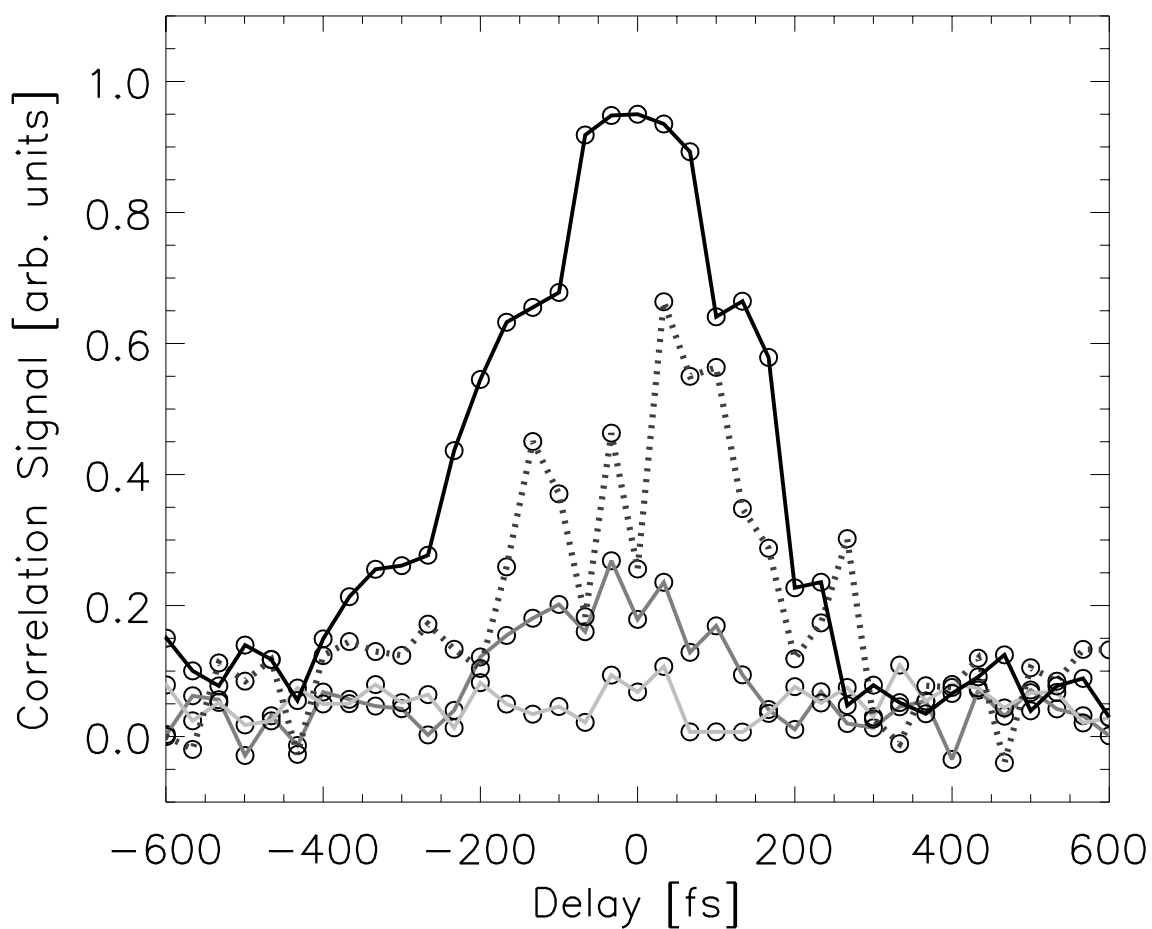


Figure 7.8: Time traces of the cross-correlation features in the Br_2 data (400 nm pump and 17th harmonic probe). Black line: signal from the ATI process leaving the Br_2^+ ion in the ground X state. Dark gray line: signal from the ATI process leaving the Br_2^+ ion in the excited A state. Medium gray line: transient signal from ionization of the excited state wavepacket. Light gray line: random background noise.

less energy is available to the electrons. Figure 7.9 shows similar time traces obtained using the 19th harmonic as a probe. Again, the transient time trace is observed to rise above the noise level with a similar shape as the cross-correlation features.

As mentioned earlier in the chapter, there are two competing two-photon processes; (1) ATI where the harmonic ionizes Br_2 followed by adding one 400 nm photon above the ionization threshold, and (2) the promotion of the excited state wavepacket by the 400 nm pulse followed by ionization with the harmonic. These are indistinguishable at $t = 0$, as the photoelectron possesses the same energy. If the excited wavepacket from process (2) slides out on the dissociative curve and is then ionized, however, the photoelectron peak will appear at a lower photoelectron energy. This is feasible if the wavepacket quickly falls down the steeply sloped section of the dissociative curve and then moves slowly in comparison when reaching the flatter section. The position of the transient photoelectron peak (Fig. 7.3) indicates that the wavepacket is ionized at an energy of $\sim 17000 \text{ cm}^{-1}$ on the $^1\Pi_u$ curve. Looking at the shape of the curve in Fig. 7.7(a), it is reasonable to assume that the wavepacket quickly falls down the steep slope from 25000 cm^{-1} to 18000 cm^{-1} , and is then ionized from the flatter part of the curve.

Scans averaged over a larger number of laser pulses per time step were also taken of this transient signal from time delays of -33 fs to +165 fs with the 19th harmonic as a probe. The relevant part of the photoelectron spectrum for these time delays is shown in Fig. 7.10, as well as time traces for the ATI cross-correlations and transient state. These photoelectron spectra are plotted with photoelectron energy as the x axis instead of binding energy, as in Fig. 7.3. Again, it is clear that the transient signal (shaded region from 4.9 to 5.5 eV) rises above the random noise signal and has a structure similar to the cross-correlation features. From these time traces, as well as from Figs. 7.8 and 7.9, the peak of the transient signal is slightly delayed in time from the peak of the cross-correlation traces. This is also consistent with the wavepacket being ionized after it has moved out on the dissociative curve with a small time delay. However, this observed delay between the peak of the cross-correlation and the peak of the transient signal time trace is very small (10-20 fs) and it is difficult to be certain of such a small time delay with

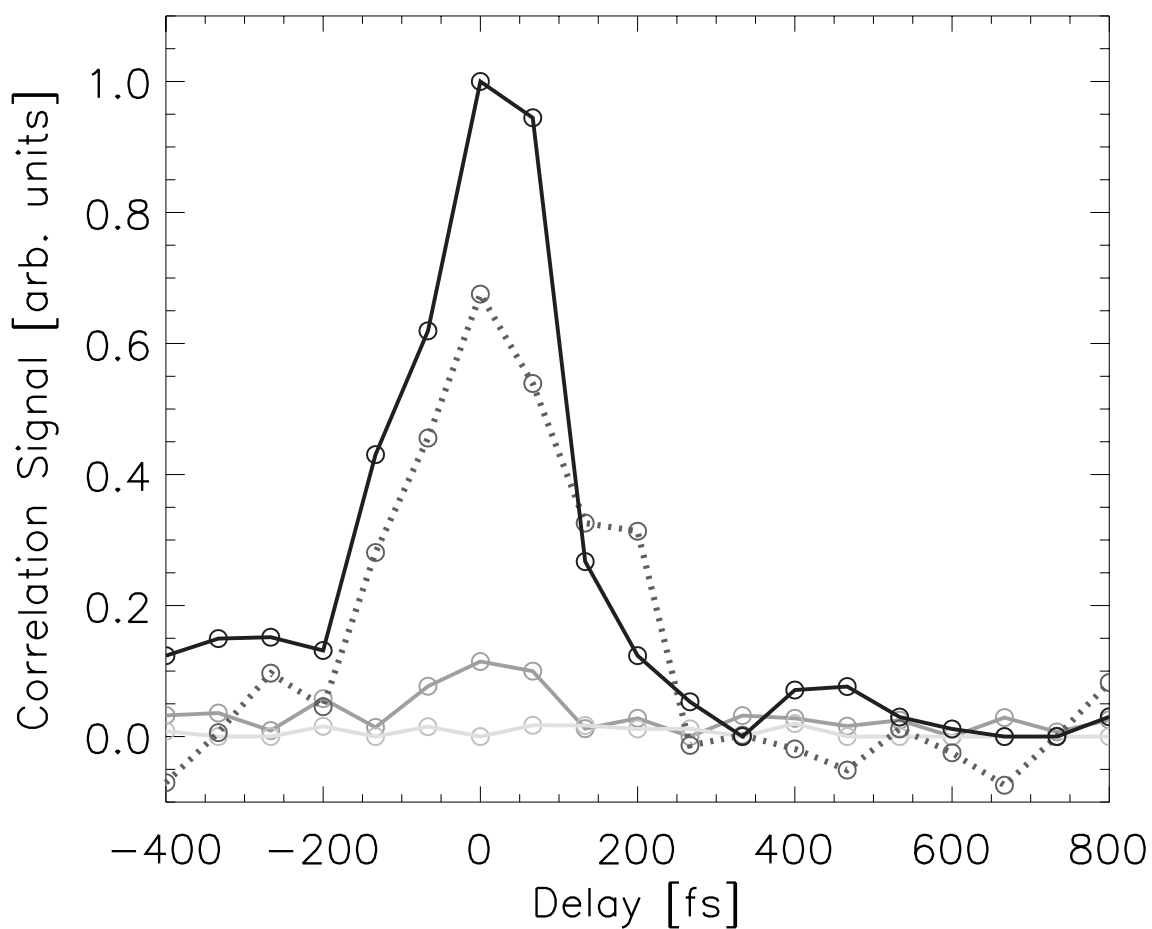


Figure 7.9: Time traces of the cross-correlation features in the Br_2 data (400 nm pump and 19th harmonic probe). Black line: signal from the ATI process leaving the Br_2^+ ion in the ground X state. Dark gray line: signal from the ATI process leaving the Br_2^+ ion in the excited A state. Medium gray line: transient signal from ionization of the excited state wavepacket. Light gray line: random background noise.

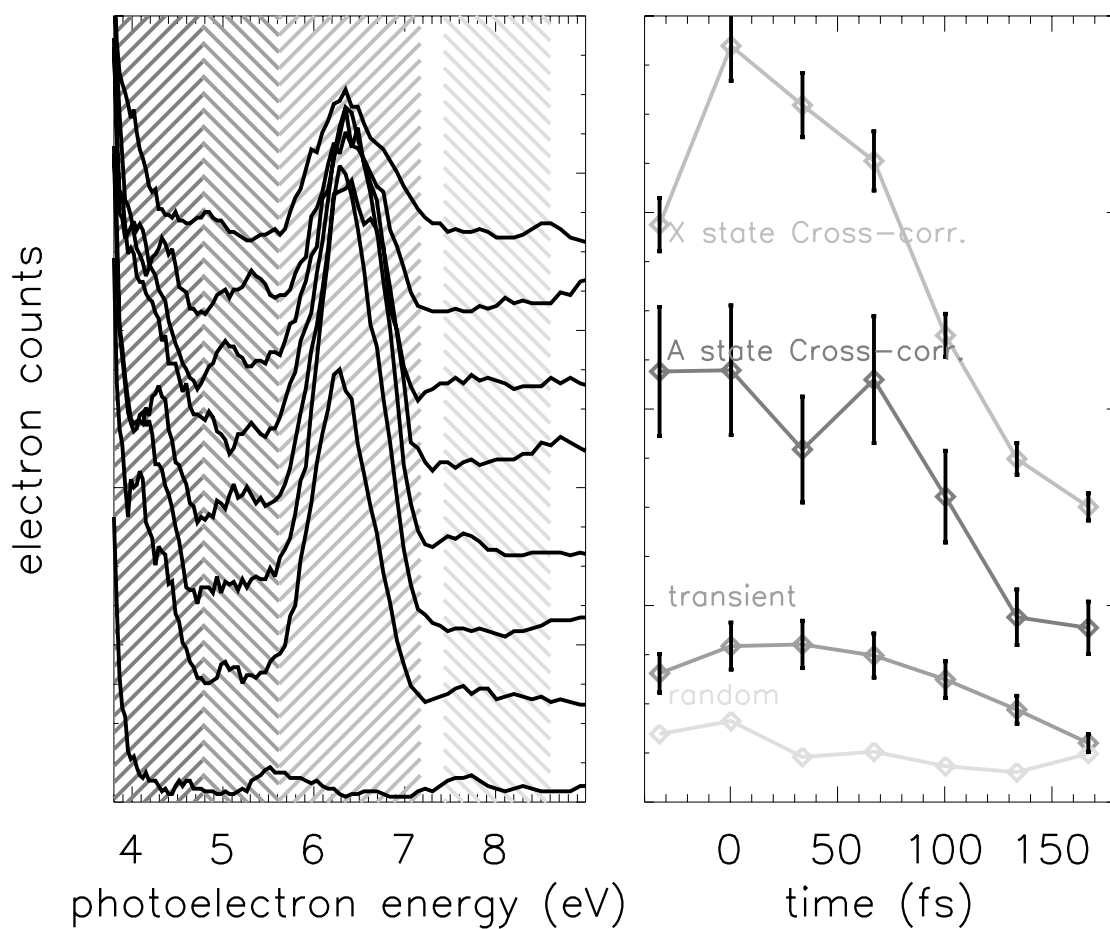


Figure 7.10: Long scans of the cross-correlation photoelectron energy region with the 19th harmonic as a probe. The shaded areas of the photoelectron spectra on the left correspond to the photoelectron energy regions giving rise to the time traces on the right. The photoelectron spectrum on the very bottom is a background, with no 400 nm pump beam, and from there the time delays step up from -33 fs to +165 fs in steps of 33 fs.

errors of ~ 10 fs.

7.5 Ionization cross-sections of atoms and transient states

Another important result is the obvious difference in the ionization cross-section between the bromine molecule and the atom at the 47 nm probe wavelength. From the reported absorption cross-section of neutral Br_2 ($5 \times 10^{-19} \text{ cm}^2$) [6] and laser energy at 400 nm, an estimated 0.02% of the molecules in the interaction region reach the excited dissociative state, leaving the rest in the ground state, as is described in the following calculations:

Percentage of molecules excited from X \rightarrow C state in Br_2

molecules in interaction region:

$$N = 5 \times 10^{-5} \text{ Torr} \times 3.26 \times 10^{16} \text{ molecules/cm}^3/\text{Torr}$$

$$N = 1.6 \times 10^{12} \text{ molecules/cm}^3$$

flux of 400 nm light:

$$E = \frac{\hbar c}{\lambda}$$

$$E = \frac{6.626 \times 10^{-34} \text{ J} \cdot \text{s} \times 3 \times 10^{10} \text{ cm/s}}{400 \times 10^{-7} \text{ cm}}$$

$$E = 5 \times 10^{-19} \text{ J/photon}$$

$$\text{photons in } 150 \mu\text{J}: = 3 \times 10^{14} \text{ photons}$$

absorption of Br_2 sample:

$$A \cong \sigma N \ell$$

$$A = 5 \times 10^{-19} \text{ cm}^2 \times 1.6 \times 10^{12}/\text{cm}^3 \times 1 \text{ cm}$$

$$A = 8 \times 10^{-7}$$

$$A \times \text{flux} = 8 \times 10^7 \times 3 \times 10^{14} \text{ photons}$$

$$A \times \text{flux} = 3.2 \times 10^8$$

% molecules in C excited state:

$$\frac{3.28 \times 10^8}{1.6 \times 10^{12}} \times 100 = \mathbf{0.02\%}$$

The counts in the atomic peaks are compared to the total counts in the A state molecular peak. Any decrease in the molecular A state signal due to the presence of the 400 nm pump beam is imperceptible, therefore it is estimated as being less than the noise level of the data (0.8% of the total A state signal-note, this number is not used in the calculation, but rather the 0.02% from above), while the atomic peak increases by $\sim 5\%$ of that same A state signal. Note, the area under the peaks in Fig. 7.2 is not representative of the total counts used in the calculation, because the A state appears compressed on the energy scale. The A state signal is in turn $\sim 30\%$ of the total signal originating from the ground state of neutral Br₂. From these numbers we can calculate the ratio of the atomic and molecular cross-section for the 17th harmonic in Br₂, as is shown in Table 7.1.

Table 7.1: A calculation of the enhancement of the atomic cross-section compared to the molecular cross-section for the 17th harmonic of 800 nm. Using 10,000 molecules as an arbitrary number, the raw photoelectron counts are used to calculate the ratio.

Br ₂ X to Br ₂ ⁺ A		Br ² P to Br ⁺ ³ P	
30%	of 10,000 mol.	0.02%	of 10,000 mol.
3,000	molecules	4	atoms
43915 ± 0.8%*	counts	2218 ± 7%†	counts
= 14.6‡	counts/molecules	= 554‡	counts/atoms
	554/14.6	~ 40	

*total counts in A state peak averaged over 10 identical scans

†total counts in atom peaks averaged over 5 identical scans at long delay times

‡similar to cross-section (σ), assuming path length is the same

The enhancement of the atomic signal compared to the molecular signal raises interesting questions about pump-probe spectroscopy with soft x-rays. If the cross-section of the Br atoms was not enhanced, the photoelectron signal would likely be imperceptible above the background noise. From the calculated estimate of the photodissociation yield, the 17th harmonic probe wavelength is ~ 40 times more sensitive to the atoms than to the ground state molecule (taking

into account the stoichiometric ratio of Br₂ to Br). One possibility is that the 17th harmonic accidentally overlaps with a resonance that enhances the atomic cross section. To attempt to fully understand this enhancement in cross-section, several different harmonics (13-21) were used in the same pump-probe experiment. A comparison of the resulting photoelectron spectra is given in Fig. 7.11. The spectra are normalized to the background signal on either side of the atomic peaks. It is clear from Fig. 7.11 that the atomic signal increases with decreasing harmonic number, as the energy of the probe approaches the threshold for ionization.

For the photoelectron spectra in Fig. 7.11, a similar calculation was done to determine the cross-section ratio for harmonics 13-21. A problem arises, however, when comparing data from the various harmonics. The flight tube voltage varies between data sets, causing the number of total counts in the molecular A state to change due to cutting off part of the photoelectron peak. This affects the outcome of the cross-section calculation since the atomic peaks are referenced to the molecular A state peak. To ensure that the calculation of the cross-section enhancement is correct, the ratios of the counts in the molecular A state peak to the counts in the molecular X state peak were determined for the pump-probe scans and then compared to the A/X ratio for a photoelectron scan where the A state was not at the edge of the energy cutoff. Assuming the X state peak is only slightly saturating the detector, which is the case since the spin-orbit doublet is still visible, comparing these two ratios gives a correction factor. The results of these calculations are given in Table 7.2. The final cross-section enhancement factors are plotted

Table 7.2: The corrections and final values for the enhancement of the atomic cross-section compared to the molecular cross-section for harmonics 13-21.

harmonic	$\sigma_{Br}/\sigma_{Br_2}$	error*	correction factor	final $\sigma_{Br}/\sigma_{Br_2}$
13	113.17	5.46	2.02	56.1
15	84.25	1.61	1.73	48.8
17	53.65	4.91	1.16	46.1
19	60.33	1.64	2.35	25.7
21	65.20	0.81	3.00	21.7

*based on the error from averaging several scans with identical detector and flight tube voltage settings, as well as the pressure of Br₂

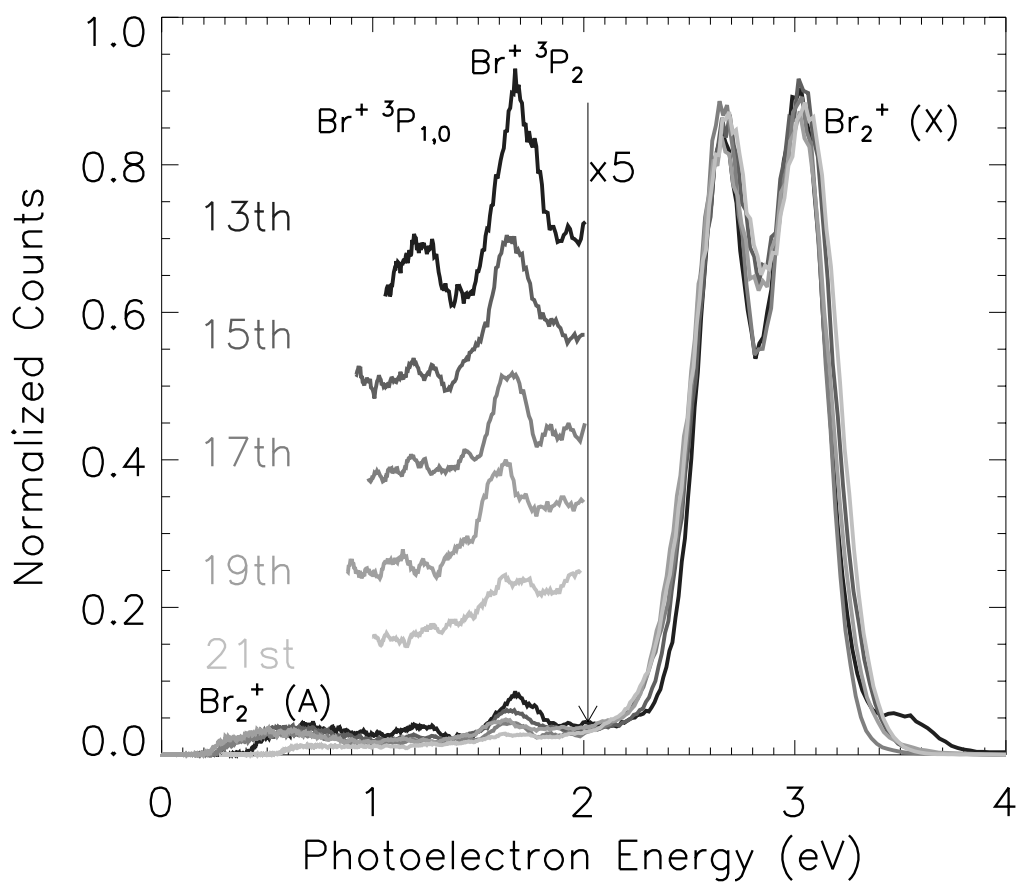


Figure 7.11: Photoelectron spectra of Br_2 at long time delays, after the atomic signal between 1 and 2 eV photoelectron energy has reached a maximum value. The atomic signal clearly increases as the harmonic number decreases. (The background signal in the vicinity of the atomic peaks is used for normalization.)

versus harmonic photon energy in Fig. 7.12. The trend in Fig. 7.12 is consistent with the trend observed in Fig. 7.11, further supporting the calculation of the cross-section enhancement. This figure also demonstrates that the 17th harmonic probe energy was not hitting a resonance in the ionization cross-section for Br, but that the cross-section is similarly enhanced for neighboring harmonics (although to varying degrees). It is also important to notice that even though the atomic signal is enhanced by a factor of ~ 20 for the 21st harmonic, it is barely visible above the background noise.

An important scientific question is whether the cross-section of the dissociative molecular state is similarly enhanced. If not, a broad signal originating from the dissociative state of the molecule in the atomic photoionization energy region may be easily obscured. Similarly, cross-correlation features from the above threshold ionization process can mask photoelectron signals arising from transient states. For three different scans where the transient signal (discussed in section 7.4) was observed, the percentage of the total two-photon signal around $t=0$ of each type of signal (ATI signal leaving the Br_2^+ in the X and A states, as well as the transient signal from ionization of the excited state wavepacket) is calculated in Table 7.3. Interestingly,

Table 7.3: The percentages by total counts of the cross-correlation and transient photoelectron signals for three different scans and two probe wavelengths.

scan	Figure	% X ATI	% A ATI	% X transient*
17th + 400 nm	7.8	53.9	33.1	13.0
19th + 400 nm	7.9	56.6	34.7	8.6
19th + 400 nm	7.10	54.4	33.2	12.4

*%of the sum of X state and A state ATI signals and transient signal arising from the intermediate neutral excited state (or total two-photon molecular signal)

the fraction of transient signal does not change dramatically when going from the 17th to the 19th harmonic, while the atomic cross-section is reduced by a factor of 2 from the 17th to the 19th. This points to the possibility that the cross-sectional enhancements might be different for transient states than for the final atomic products. This type of information is crucial when attempting to measure the time dynamics of transient states.

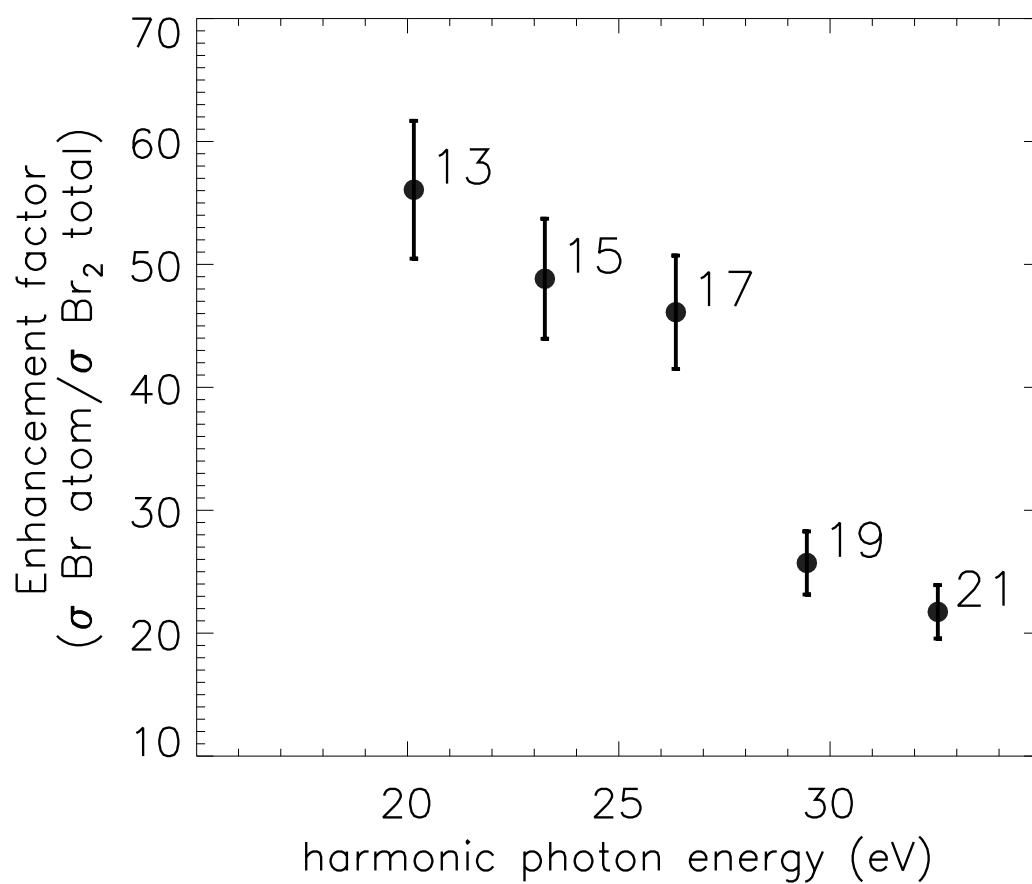


Figure 7.12: The cross-section enhancement factor plotted vs. the harmonic photon energy, demonstrating that the 17th harmonic probe was not sitting on a resonance for atomic Br, but the atom signal is similarly enhanced for several harmonics.

7.6 Conclusions

In a simple molecule like Br_2 , we demonstrate the many factors that come into play when measuring ionization from excited states and excited state photodissociation dynamics. These issues have important implications for future pump-probe spectroscopies, specifically with soft x-rays. Electron distributions from excited neutral to ion states, the complication of above threshold ionization features in time-resolved spectroscopy, the time-dependent appearance of atomic photoelectron signals, the enhancement of ionization cross-sections of atomic species vs. molecular species, and the shapes and cross-sections of signals arising from excited transient states are all relatively unexplored phenomena. For neutral gas phase species, UV/visible-pump soft x-ray probe photoelectron spectroscopy proves to be a powerful tool for probing dissociation and excited state dynamics, both in the nanosecond and femtosecond regime.